

## Supporting Information

### **MOF-assisted Antifouling Material: Application in Rapid Determination of TB gene in Whole-serum Specimens**

Chenhui Wu <sup>1</sup>, Yunkang Ma <sup>1</sup>, YingxiaZhou, Wenjie Yang, LihuaChen \*

Key Laboratory of Optic-electric Sensing and Analytical Chemistry for Life Science; Shandong Key Laboratory of Biochemical Analysis; Key Laboratory of Analytical Chemistry for Life Science in Universities of Shandong; Key Laboratory of Eco-chemical Engineering; College of Chemistry and Molecular Engineering, Qingdao University of Science and Technology, Qingdao 266042, PR China.

<sup>1</sup> These authors contributed equally to this work.

\*Corresponding author: Lihua Chen, E-mail: Lihuachen@qust.edu.cn, Fax: +86 53284022681; Tel: +86 15054246089

**Table.S1.** Sequences of the oligonucleotides used in this study

---

<b>Name</b>	<b>Sequence (5'→3')<sup>a</sup></b>
<b>TB–probe1</b>	NH <sub>2</sub> -(CH <sub>2</sub> ) <sub>6</sub> -CAGCGCCGACAGTCGGCG CTTGTGGGTCAACCCCGA
<b>TB–target</b>	TCGGGGTTGACCCACAAGCGCCGACTGTCTG GCGCTG
<b>TB-one-base mismatch (M1-1)</b>	TCGGGGTTGACCT <u>T</u> ACAAGCGCCGACTGTCTG GCGCTG
<b>TB -two-base mismatch (M2-1)</b>	TCGGGGTTGACCT <u>TA</u> ACAAGCGCCGACTGT <u>TG</u> GCGCTG
<b>TB-three-base mismatch (M3-1)</b>	TCGGGGTTGACCT <u>TACA</u> AGCGCCGACTGT <u>GT</u> GCGCTG
<b>TB-complete mismatch (WB)</b>	<u>GATTTTGGTCAAACACCTATAATCAGTGA</u> <u>TTATAGT</u>

---

Sequences of the oligonucleotides used in this study were designed in a BLAST search of GenBank DNA sequences (<http://www.ncbi.nlm.nih.gov/Genbank/index.html>). And we found no homology with genes of other diseases.

## Experimental Section

### 1.1. Preparation of $\text{NH}_2\text{-MIL-53 (Al)}$

$\text{NH}_2\text{-MIL-53 (Al)}$  was prepared according to the reported method<sup>1</sup>. Firstly, the mixture solution of 33.7 mL  $\text{N,N}$ -Dimethylformamide (DMF) and 11.2 mL water containing 1.14 g  $\text{AlCl}_3 \cdot 6\text{H}_2\text{O}$  and 0.840 g 2-Aminoterephthalic Acid ( $\text{NH}_2\text{-BDC}$ ) was put into a 80.0 mL Teflon-lined stainless steel autoclave and reacted for 24 h at  $150^\circ\text{C}$  in oven. After vacuum filtration, the product was dissolved in DMF and refluxed for 8 hours at  $150^\circ\text{C}$ . Next, the product was washed by acetone through filtering to remove free DMF from the channels. Finally, the product was dissolved in DMF again and diluted to  $10.0 \text{ mg mL}^{-1}$  with 10.0 mM Tris-HCl ( $\text{pH}=8.00$ ) and put into refrigerator at  $4^\circ\text{C}$  for the further use.

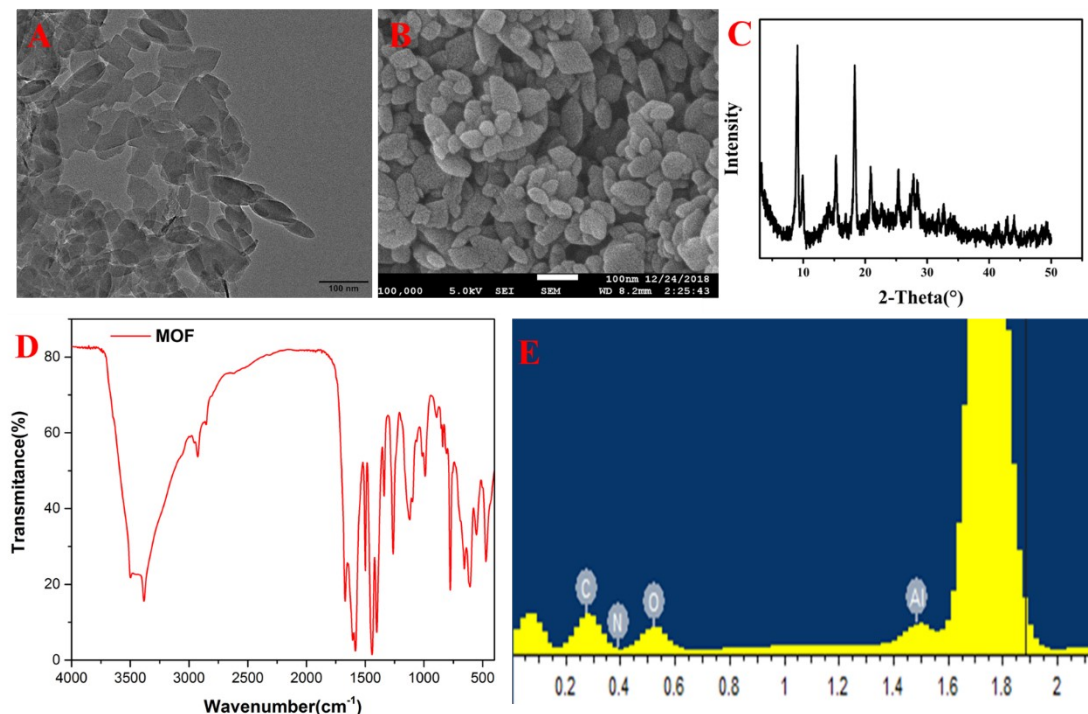


**Fig.S1.**, TEM image (A), SEM image (B), X-ray diffractograms (C), FTIR (D), and EDS (E) of  $\text{NH}_2\text{-MIL-53 (Al)}$ .

TEM and SEM were both used to estimate the size and morphology of the NH<sub>2</sub>-MIL-53 (Al). As shown in Fig.S1A (TEM) and Fig.S1B (SEM), the ellipsoidal and rhomboidal shape of NH<sub>2</sub>-MIL-53 (Al) with uniform size about  $70 \pm 10$  nm is observed. Additionally, XRD pattern of NH<sub>2</sub>-MIL-53 (Al) is shown in Fig.S1C. There are two stronger characteristic diffraction peaks at 9.20 and 18.2, which corresponded to the (110), (211) and (220) crystal planes, respectively. Moreover, several characteristic peaks were exhibited in FTIR spectrum (Fig. S1D).  $3437\text{ cm}^{-1}$  and  $3386\text{ cm}^{-1}$  are correspond to NH<sub>2</sub> group,  $1583\text{ cm}^{-1}$  and  $1497\text{ cm}^{-1}$  to asymmetric stretching of carbonyl,  $1443\text{ cm}^{-1}$  and  $1404\text{ cm}^{-1}$  to symmetric stretching of carbonyl,  $2918\text{ cm}^{-1}$  and  $2849\text{ cm}^{-1}$  to symmetrical stretching and asymmetrical stretching vibration of the methyl group (Fig.S1D). Finally, as shown in Fig.S1E, Al, O, C, N elements were existed in EDS of MOF. All results are consistent with that reported in the other literature, indicating the successful construction of NH<sub>2</sub>-MIL-53 (Al) <sup>1,2</sup>.

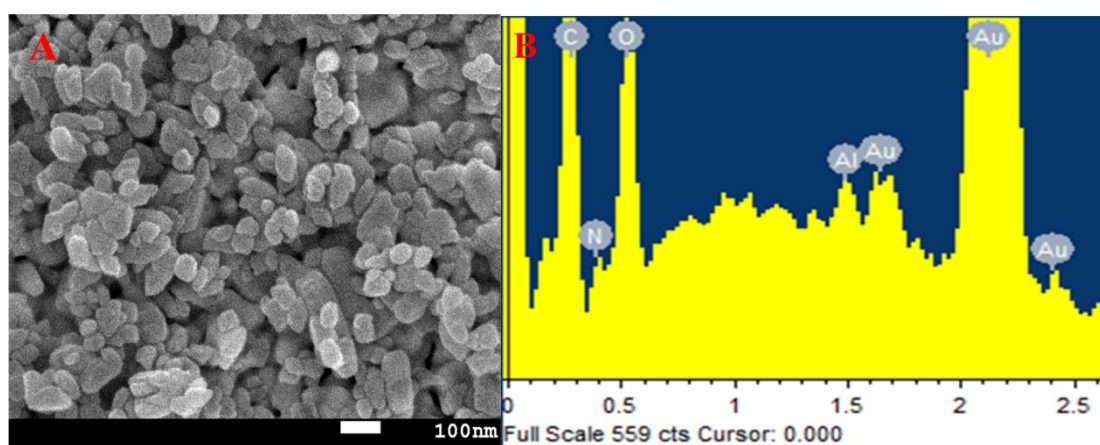


**Fig.S2.** SEM image (A) and EDS (B) of MOF/Au NPs.

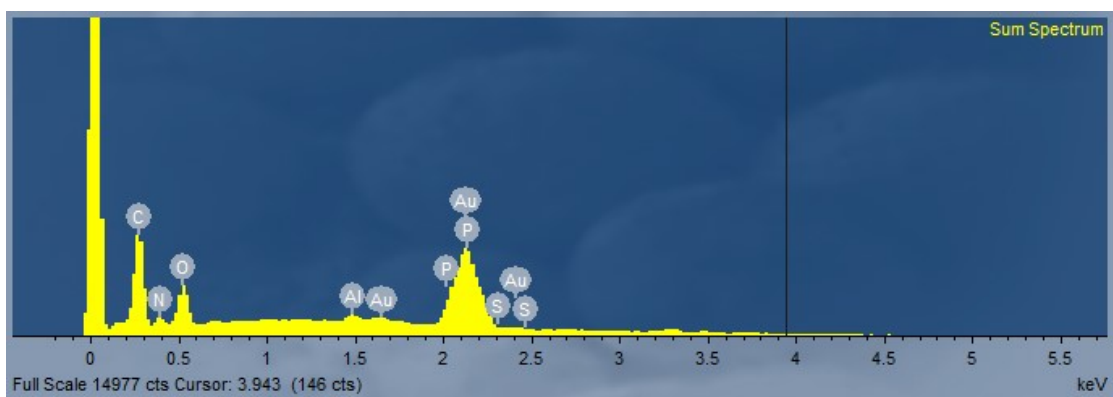


**Fig.S3.** EDS spectra of interface probe/CS@MOF/Au NPs/GCE.

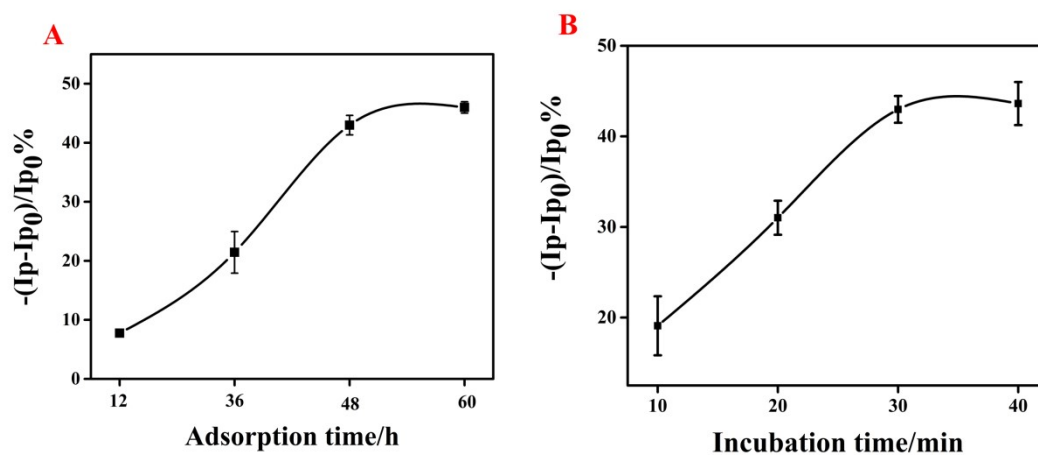


**Fig.S4.** Effect of the adsorption time of CS (A) and incubation time (B) on the DPV responses of the biosensor toward  $1.00 \times 10^{-11}$  M target DNA.

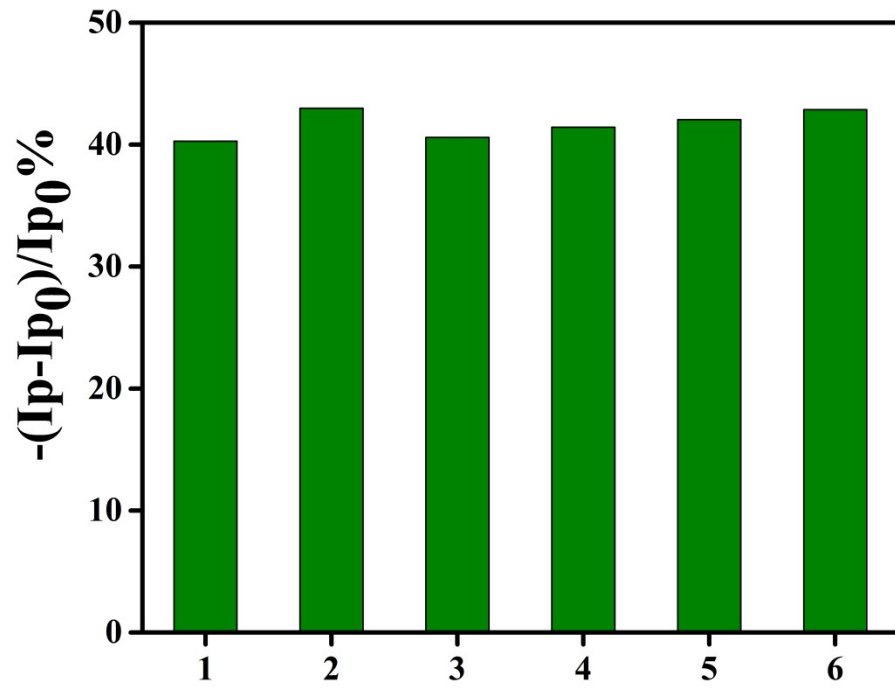


Fig.S5. The reproducibility of the electrochemical TB biosensor.

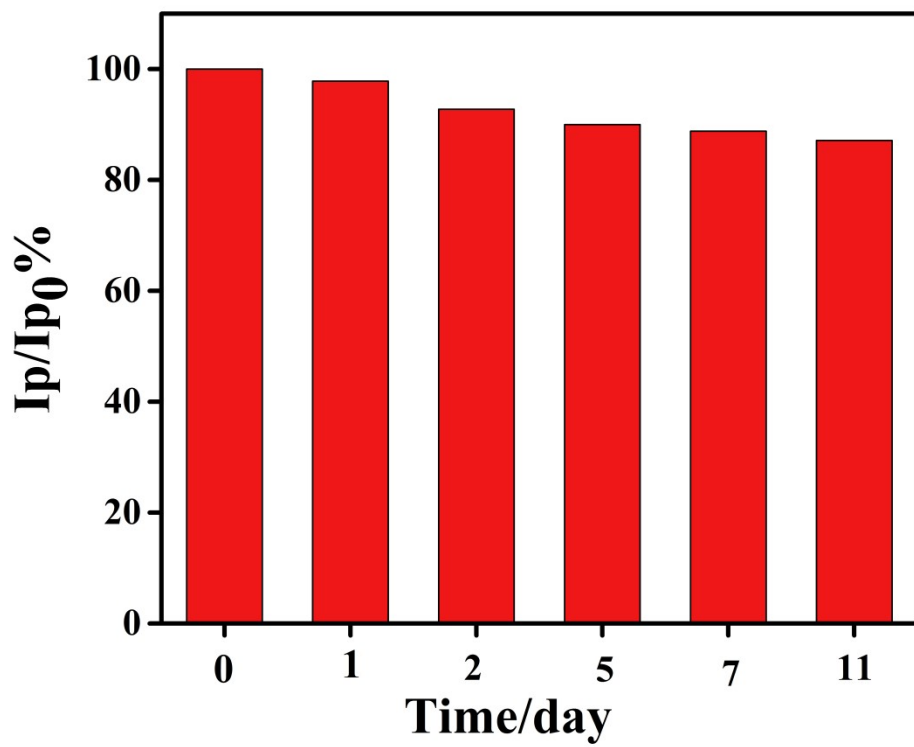
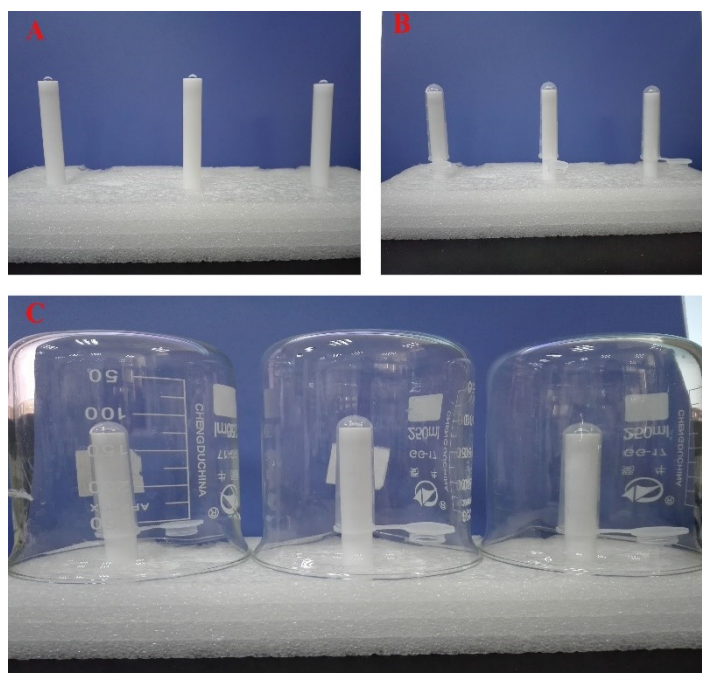
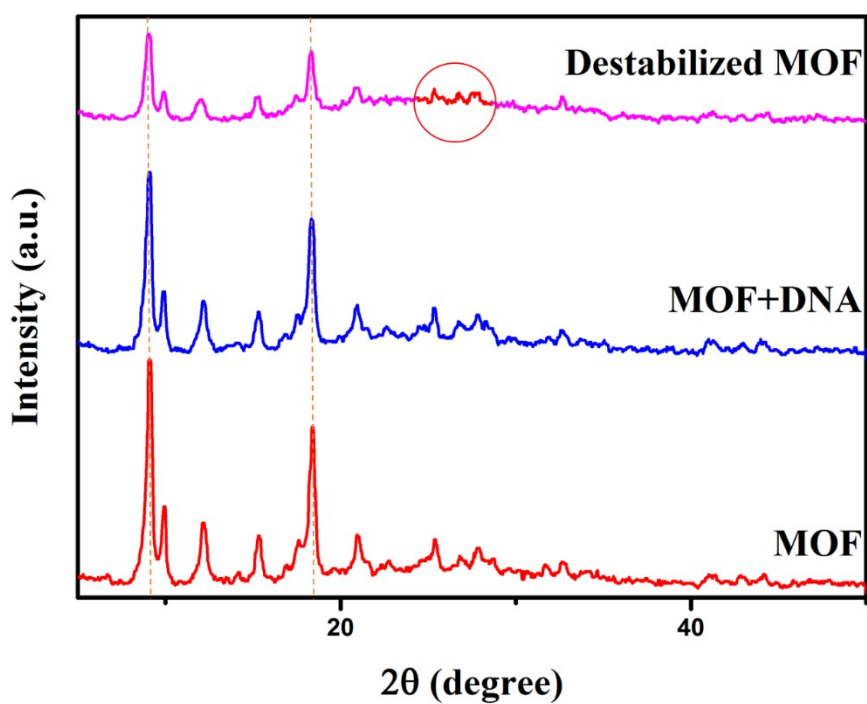


Fig.S6. The time stability study of the TB biosensor.



**Fig.S7.** A: Glassy carbon electrodes drop-coated with antibody solution; B: Glassy carbon electrodes covered with round-bottomed centrifuge tubes; C: Glassy carbon electrodes covered with round-bottomed centrifuge tubes and glass beakers.



**Fig.S8.** The XRD pattern of MOF, MOF+ DNA (MOF incubated in Probe DNA) and

destabilized MOF

Fig.S8 provides the XRD pattern of MOF, MOF+ DNA and destabilized MOF. The diffraction peaks of MOF match well with the simulated patterns calculated from the corresponding crystallographic data. This indicates that the synthesized MOF is phase-pure. After the incubation in probe DNA, MOF+ DNA maintain the peaks of MOF, suggesting the well preservation of crystalline characters of MOF. As we can see, for the destabilized MOF, peaks at  $2\theta$  of  $9.2^\circ$  and  $18.2^\circ$  decrease very much. In addition, peaks at  $2\theta$  of  $25.4^\circ$  and  $27.8^\circ$  basically disappeared. Therefore, the crystal structure of MOF is stable in the presence of DNA.

**Table.S2.** Analytical results for target DNA in 100% serum.

Samples	Added (fM)	Found (fM)	Recovery (%)	RSD (%)
1	1.000	1.010	101.0	10.68
2	100.0	108.2	108.2	6.430
3	1000	1036	103.6	1.390

### **The discussion of Table 1 in manuscript**

From Table 1 in manuscript, all TB biosensors constructed by several materials



demonstrated the relatively good analytical characteristics. For example, the electrode modified with CNTs-PAN has a wide linear range from  $10^{-15}$  M to  $10^{-8}$  M and a low limit of detection (0.330 fM). However, these excellent properties are only demonstrated in buffer. Compared with them, the biosensor based on CS@MOF shows a wider linear range from  $10^{-16}$  M to  $10^{-11}$  M and a lower limit of detection (30.0 aM) not only in buffer, but also in 100% serum.

### Data acquisition and processing

**Fig.4A in manuscript:** The DPV responses of three electrodes (CS@MOF/Au NPs/GCE) prepared independently were collected respectively. The ordinate (Y) is the

mathematical average of the change rate of the DPV  $\left( Y_i = \frac{|(I_p - I_{p0})|}{I_{p0}} \times 100\% \right)$ .

DPV responses before the incubation in 100% serum ( $I_{p0}$ ), DPV responses after the incubation in 100% serum ( $I_p$ ) and the label of the measured electrode (i).

**Fig.4B in manuscript:** The DPV responses of three electrodes prepared independently were collected respectively. The ordinate (Y) is the mathematical

average of the change rate of the DPV  $\left( Y_i = \frac{|(I_p - I_{p0})|}{I_{p0}} \times 100\% \right)$ , expressed by

equation:  $Y = \frac{(Y_1 + Y_2 + Y_3)}{3}$ . The error bar:  $\pm SD = \sqrt{\frac{1}{n-1} \sum (Y_i - Y)^2}$ . DPV

responses before the incubation in various media ( $I_{p0}$ ), DPV responses after the incubation in various media ( $I_p$ ), the total number of electrodes prepared independently (n) and the label of the measured electrode (i).

**Fig.4C and 4D in manuscript:** The contact angles of each modified interface of

three electrodes (CS@MOF/Au NPs/ITO) prepared independently were collected respectively. The contact angles for each modified interface of the electrodes is expressed by equation:  $\bar{Z} \pm SD$ , the average value of contact angle:  $\bar{Z} = \frac{(\angle_1 + \angle_2 + \angle_3)}{3}$ , the error bar:  $\pm SD = \sqrt{\frac{1}{n-1} \sum (\angle_i - \bar{Z})^2}$ , the total number of electrodes prepared independently (n) and the label of the measured electrode (i),  $\angle$  is the data measured by JC2000C1 goniometer.

**Fig.5C and 5D in manuscript:** Three electrodes prepared independently were used for the detection of each sample, DPV responses before the hybridization ( $I_{p0}$ ), DPV responses after the hybridization ( $I_p$ ), the total number of electrodes prepared independently (n) and the label of the measured electrode (i). The ordinate (Y) is the

mathematical average of the change rate of the DPV  $\left( y_i = \frac{|(I_p - I_{p0})|}{I_{p0}} \times 100\% \right)$ ,

expressed by equation:  $\bar{y} = \frac{(y_1 + y_2 + y_3)}{3}$ . The error bar:

$\pm SD = \sqrt{\frac{1}{n-1} \sum (y_i - \bar{y})^2}$ .  $x = \log_{10} C$ , C is the concentration of the added target

DNA. The equation is  $\bar{x} = \frac{(x_1 + x_2 + x_3)}{3}$ .  $\hat{b} = \frac{\sum_{i=1}^n x_i y_i - n \bar{x} \bar{y}}{\sum_{i=1}^n x_i^2 - n \bar{x}^2}$  and the formula of

the liner fitting is expressed by equation:  $\hat{y} = \hat{b}x + \hat{a}$ .

**Fig.6 in manuscript:** The calculation method of ordinate for Fig.6 is the same as that for Fig 4A and 4B. Three electrodes prepared independently were used for the detection of each sample. DPV responses before the hybridization ( $I_{p0}$ ), DPV responses

after the hybridization ( $I_p$ ), the total number of electrodes prepared independently ( $n$ ) and the label of the measured electrode ( $i$ ).

## References

- 1 X. Cheng, A. Zhang, K. Hou, M. Liu, Y. Wang, C. Song, G. Zhang and X. Guo, Size- and morphology-controlled  $\text{NH}_2$ -MIL-53(Al) prepared in DMF–water mixed solvents, *Dalton Trans.*, 2013, **42**, 13698–13705. <https://doi.org/10.1039/c3dt51322j>.
- 2 L. Liu, X. Tai, X. Zhou and L. Liu, Synthesis, post-modification and catalytic properties of metal-organic framework  $\text{NH}_2$ -MIL-53(Al), *Chem. Res. Chin. Univ.*, 2017, **33**, 231–238. <https://doi.org/10.1007/s40242-017-6420-7>.